

Chi Wu*

Shuiqin Zhou
Department of Chemistry
The Chinese University of
Hong Kong
Shatin, N.T., Hong Kong

Wei Wang

Polymer Physics Laboratory
Changchun Institute of Applied
Chemistry
Academia Sinica
Changchun, 130022, China

A Dynamic Laser Light-Scattering Study of Chitosan in Aqueous Solution

The solution behavior of four chitosans (91% deacetylated chitin) with different molecular weights in 0.2M CH₃COOH/0.1M CH₃COONa aqueous solution was investigated at 25°C by dynamic laser light scattering (LLS). The Laplace inversion of the precisely measured intensity-intensity time correlation function leads us to an estimate of the line-width distribution G(Γ), which could be further reduced to a translational diffusion coefficient distribution G(D). By using a combination of static and dynamic LLS results, i.e., M_w and G(D), we were able to establish a calibration of D = k_DM^{- α_D} with k_D = (3.14 ± 0.20) × 10⁻⁴ and α_D = 0.655 ± 0.015. By using this calibration, we successfully converted G(D) into a molecular weight distribution f_w(M). The larger α_D value confirms that the chitosan chain is slightly extended in aqueous solution even in the presence of salts. This is mainly due to its backbone and polyelectrolytes nature. As a very sensitive technique, our dynamic LLS results also revealed that even in dilute solution chitosan still forms a small amount of larger sized aggregates that have been overlooked in previous studies. The calibration obtained in this study will provide another way to characterize the molecular weight distribution of chitosan in aqueous solution at room temperature.
© 1995 John Wiley & Sons, Inc.

INTRODUCTION

Chitosan, partially deacetylated chitin, is an important kind of natural biopolymer composed mainly of two kinds of common sugars, 2-acetamino-2-deoxy-D-glucose (N-acetyl-D-glucosamine) and 2-amino-2-deoxy-D-glucose (D-glucosamine). Usually, chitin can be extracted from the outer shell of the crustaceans, shrimp and crab.¹ Due to its unique solution, chemical, physical, and biolog-

ical properties, especially its biocompatibility and its ability to form films, fibers, and gels, chitosan has already been extensively used in a variety of biomedical applications, such as bacteriostatic agent, contact lens, wound dressings, and immunoadjuvant, to name but a few.

As a linear polyelectrolyte, chitosan has both reactive amino groups and hydroxyl groups. Its physical and solution properties changes with the sur-

Received May 18, 1994; accepted September 9, 1994.

* To whom correspondence should be addressed.

Biopolymers, Vol. 35, 385-392 (1995)

© 1995 John Wiley & Sons, Inc.

CCC 0006-3525/95/030385-08

rounding chemical environment. When the pH value is less than 6.5, chitosan in solution carries a positive charge along its backbone. It is this cationic nature that makes it possible to be used in many biomedical applications because it can be attracted, or say, bound to usually negatively charged tissues, skin, bone, and hair. It is known that its binding ability depends on its chain conformation in solution and its molecular weight. Static (classic) light scattering and viscometry has been widely used in the past to investigate these molecular properties.^{2,3} A number of methods have been used to degradation of Chitosanas.⁴ The Mark-Houwink equations for chitosans with different degrees of deacetylation have been established.⁵ High-resolution nmr was used to determine the acetylation sequences, the degree of *N*-acetylation, and the distribution of *N*-acetyl groups in chitosan.^{6,7} However, mainly due to its polyelectrolyte nature, the characterization of molecular weight distribution of chitosans in aqueous solution has been hindered.

Recently, dynamic laser light scattering (LLS) as a newly established analytical method has found its application in the characterization of various special types of macromolecules including polyelectrolytes, such as dextran⁸ and gelatin.⁹ The advantage of using dynamic LLS over other methods are mainly attributed to the following aspects: first, it can analyze macromolecules in hostile conditions, such as in strong acid and at high temperature; second, its calibration depends only on the type of solvent and temperature, but not on a particular LLS instrument; third, it is a nondestructive method.

It is our objective in this study to establish a calibration between the measured translational diffusion coefficient D in dynamic LLS and molecular weight M . This calibration is directly related to the chain conformation of chitosan in aqueous solution. With this calibration, we are able to calculate the molecular weight distribution $f_w(M)$ from the translational diffusion coefficient distribution $G(D)$ measured in dynamic LLS.

BASIC THEORIES

Static Light Scattering

The angular dependence of the excess absolute time-averaged scattered intensity, known as the excess Rayleigh ratio [$R_w(\theta)$], was measured. For a

dilute solution at concentration C (g/mL) and the scattering angle θ , $R_w(\theta)$ can be approximately expressed as¹⁰

$$\frac{KC}{R_w(\theta)} \cong \frac{1}{M_w} \left(1 + \frac{1}{3} \langle R_g^2 \rangle q^2 \right) + 2A_2C \quad (1)$$

where $K = 4\pi^2 n^2 (dn/dC)^2 / (N_A \lambda_0^4)$ and $q = (4\pi n / \lambda_0) \sin(\theta/2)$ with N_A , dn/dC , n , and λ_0 being Avogadro's number, the specific refractive index increment, the solvent refractive index, and the wavelength of light in vacuo, respectively. M_w is the weight average mass of dissolved polymers; A_2 , the second-order virial coefficient; and $\langle R_g^2 \rangle^{1/2}$, or simply R_g , the rms z -average radius of polymer. By measuring $R_w(\theta)$ at a set of C and θ , we are able to determine M_w , R_g , and A_2 from a Zimm plot that incorporates the dependence of $KC/R_w(\theta)$ on both C and θ in a single grid.¹⁰

Dynamic Light Scattering

An intensity-intensity time correlation function $G^{(2)}(n\Delta\tau, \theta)$ in the self-beating mode is normally measured, which has the following form^{11,12}:

$$\begin{aligned} G^{(2)}(t, \theta) &= \langle I(t, \theta) I(0, \theta) \rangle \\ &= A [1 + \beta |g^{(1)}(t, \theta)|^2] \end{aligned} \quad (2)$$

where A is a measured baseline; β , a parameter depending on the coherence of the detection; t , the delay time; and $|g^{(1)}(t, \theta)|$, the normalized first-order electric field time correlation function. $|g^{(1)}(t, \theta)|$ is related to the line-width distribution $G(\Gamma)$ by

$$\begin{aligned} |g^{(1)}(t, \theta)| &= \langle E(t, \theta) E^*(0, \theta) \rangle \\ &= \int_0^\infty G(\Gamma) e^{-\Gamma t} d\Gamma \end{aligned} \quad (3)$$

$G(\Gamma)$ can be calculated from $|g^{(1)}(t, \theta)|$ by Laplace inversion. Γ normally depends on both C and θ as^{13,14}

$$\frac{\Gamma}{q^2} = D(1 + k_d C) (1 + f \langle R_g^2 \rangle q^2) \quad (4)$$

where k_d is the diffusion second virial coefficient and f is a dimensionless number. At $C \rightarrow 0$ and $\theta \rightarrow 0$, $\Gamma/q^2 \rightarrow D$.

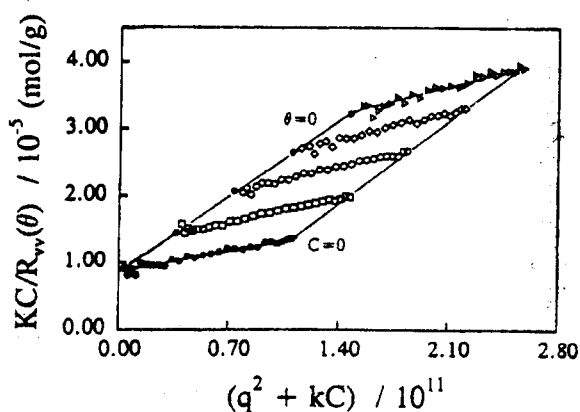


FIGURE 1 Typical Zimm plot of chitosan 4 in 0.2M $\text{CH}_3\text{COOH}/0.1\text{M}$ CH_3COONa aqueous solution at 25°C.

EXPERIMENTAL METHODS

Sample Preparation

The method of cleaning and extracting chitin from Crabshells can be found elsewhere.⁴ Chitosan with 91% deacetylation was obtained by heating dried chitin in a NaOH solution (47% w/w) at 62°C under nitrogen atmosphere. The exact degree of deacetylation was determined by the colloid titration method¹⁵ and by ir spectroscopy (Model PE-580B) method.¹⁶ Chitosans with the same degree of deacetylation, but different molecular weights, were obtained in a hydrolytic degradation of chitosan chain in acid solution of acetic acid (20% v/v) under nitrogen atmosphere at 70°C. The solutions after hydrolysis at different time were treated with NaOH solution and acetone. The longer the time, the lower the molecular weight of chitosan will be. Four such obtained chitosans were obtained and used in this study. They are labeled as chitosan 1–4 thereafter. All LLS chitosan aqueous solutions were prepared by first dissolving a certain amount of chitosan in 0.2M $\text{CH}_3\text{COOH}/0.1\text{M}$ CH_3COONa aqueous solution, and then clarified with a 0.5 μm Millipore filter in order to remove dust.

Laser Light Scattering (LLS).

A commercial LLS spectrometer (ALV/SP-125 together with an ALV-5000 digital time correlator, Langen in Hessen, Germany) was used with an argon-ion laser (Coherent INNOVA 90, operated at 488 nm and 100 mW) as light source. The primary beam is vertically polarized. In our present setup, the value of β is about 0.85, which is rather high for an LLS spectrometer capable of doing both static and dynamic LLS measurements, so that we are able to do dynamic LLS in a very dilute solution. The detail of LLS instrumentation and theory can be found elsewhere.^{11,12} All LLS measurements were done at $25.0 \pm 0.1^\circ\text{C}$. All measured time correlation functions were analyzed by the Laplace inversion program (CONTIN) equipped with the correlator.

Specific Refractive Index Increment (dn/dc)

It is vital in static LLS to have a precise value of dn/dc , since the measured M_w is proportional to $(dn/dc)^{-2}$. Recently, a novel differential refractometer was designed and constructed in our laboratory.¹⁷ The whole refractometer mounted on a small optical rail is only 40 cm in length, 10 cm in width, and 15 cm in height, which can be incorporated into any existing LLS spectrometer, wherein the laser, the thermostat, and the computer are shared, which enables us to measure the refractive index increment and the scattered light intensity under the identical experimental conditions, so that the wavelength correction is eliminated. After equilibrium dialysis, the measured dn/dc of the 91% deacetylated chitosan in 0.2M $\text{CH}_3\text{COOH}/0.1\text{M}$ CH_3COONa aqueous solution at 25°C and 488 nm is 0.190 ± 0.001 . It is slightly lower than the reported value of 0.194 at 25°C and 436 nm,⁴ which is very reasonable since $dn/dc \propto \lambda^{-2}$.

RESULTS AND DISCUSSION

Figure 1 shows a typical Zimm plot of Chitosan 4 in 0.2M $\text{CH}_3\text{COOH}/0.1\text{M}$ CH_3COONa aqueous

Table I Summarization of Light Scattering Results of Four 91% Deacetylated Chitosans in Aqueous Solution at 25°C

Sample	$10^{-5} M_w$ (g/mol)	$10^3 A_2$ (mol·mL/g ²)	R_g (nm)	$10^8 \bar{D}$ (cm ² /s)	\bar{R}_h (nm)	R_g/\bar{R}_h
Chitosan 1	3.45	7.6	82.5	5.90	40.2	2.0
Chitosan 2	2.46	6.0	58.5	7.10	34.4	1.7
Chitosan 3	1.57	4.7	47.4	9.35	25.9	1.8
Chitosan 4	1.06	6.0	34.4	12.7	19.2	1.9

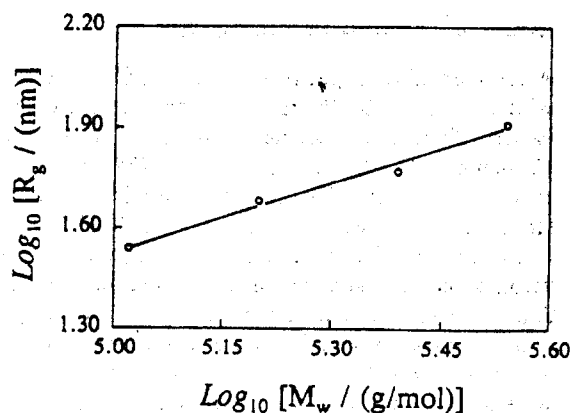


FIGURE 2 Plot of R_g vs M_w , where the line represents a least-square fitting of $R_g(\text{nm}) = 2.4 \times 10^{-2} M_w^{0.64}$.

solution at 25°C, where C is in the range of 0.496–1.98 mg/mL. On the basis of Eq. (1), we were able to calculate the values of M_w , A_2 , and R_g from the extrapolation of $[KC/R_{vv}(\theta)]_{\theta \rightarrow 0, C \rightarrow 0}$, $[KC/R_{vv}(\theta)]_{\theta \rightarrow 0}$ vs C , and $[KC/R_{vv}(\theta)]_{C \rightarrow 0}$ vs q^2 , respectively. The results are summarized in Table I. The positive values of A_2 shows that the 0.2M $\text{CH}_3\text{COOH}/0.1\text{M}$ CH_3COONa aqueous solution is a good solvent for chitosan at room temperature. In comparison with a flexible polymer chain with a similar chain length in good solvent, such as polystyrene in toluene, the values of R_g are larger.¹⁸ These larger R_g values suggests that chitosans are more extended in aqueous solution. This is understandable since in acidic condition chitosan is a cationic polyelectrolyte. The repulsion of the positive charges on the amide groups along the backbone chain will certainly make a more stretched

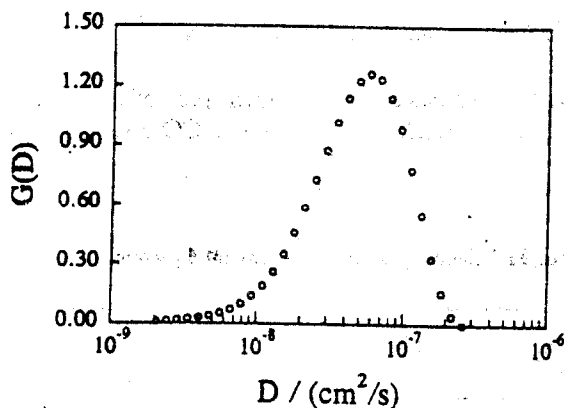


FIGURE 3 Typical diffusion coefficient distribution $G(D)$ of chitosan 4 in 0.2M $\text{CH}_3\text{COOH}/0.1\text{M}$ CH_3COONa aqueous solution at 25°C at $C \rightarrow 0$ and $\theta \rightarrow 0$.

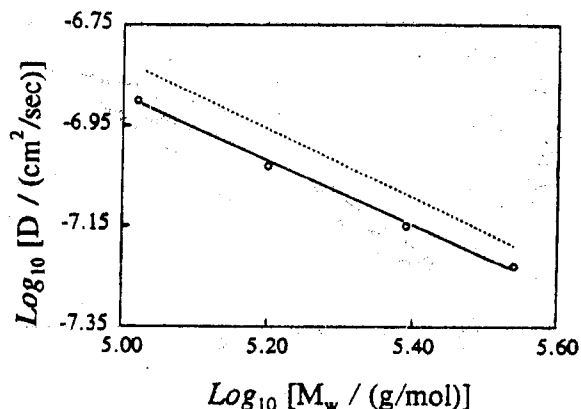


FIGURE 4 Plot of \bar{D} vs M_w , where the line shows a least-square fitting of $\bar{D}(\text{cm}^2/\text{s}) = 1.92 \times 10^{-4} M_w^{-0.64}$; and the dotted line, $D(\text{cm}^2/\text{s}) = 3.14 \times 10^{-4} M_w^{-0.665}$.

chain even though CH_3COONa as an electrolyte has been added in solution. Besides the polyelectrolyte effect, the N -acetyl groups also influence the chain conformation.¹⁹

Figure 2 shows a double logarithmic plot of R_g vs M_w . The line represents a least-square fitting of $R_g(\text{nm}) = k_R M_w^{\alpha_R}$ with $k_R = (2.4 \pm 0.2) \times 10^{-2}$ and $\alpha_R = 0.64 \pm 0.02$, which shows that chitosan has an extended chain conformation in 0.2M $\text{CH}_3\text{COOH}/0.1\text{M}$ CH_3COONa aqueous solution at 25°C, since for a flexible polymer chain in good solvent, $\alpha_R \leq 0.6$ in theory.

Figure 3 shows a typical translational diffusion coefficient distribution $G(D)$ of chitosan 4 in 0.2M $\text{CH}_3\text{COOH}/0.1\text{M}$ CH_3COONa aqueous solution at 25°C at $C \rightarrow 0$ and $\theta \rightarrow 0$. The long tail of $G(D)$ indicates that the molecular weight distribution is broad. It should be stated that $G(D)$ is a z - or intensity-weighted distribution. After having $G(D)$, we were able to calculate the z -average translational diffusion coefficient $\bar{D} [= \int_0^\infty G(D)D dD]$, and then the average hydrodynamic radius \bar{R}_h by replacing D with \bar{D} in the Stokes-Einstein equation, $R_h = k_B T / (6\pi\eta D)$ where k_B , T , and η are the Boltzmann constant, the absolute temperature, and the solvent viscosity, respectively. The calculated values of \bar{D} , \bar{R}_h , and R_g/\bar{R}_h of four chitosans are also listed in Table I. The ratios of R_g/\bar{R}_h are slightly larger than the values (1.5–1.8) observed for a flexible polymer chain in good solvent,²⁰ which further shows that chitosan has an extended chain conformation in 0.2M $\text{CH}_3\text{COOH}/0.1\text{M}$ CH_3COONa aqueous solution at 25°C.

Figure 4 shows a double logarithmic plot of \bar{D} vs M_w . The solid line shows a least-square fitting of \bar{D}

(cm^2/s) = $\langle k_D \rangle M_w^{-\langle \alpha_D \rangle}$ with $\langle k_D \rangle = (1.92 \pm 0.10) \times 10^{-2}$ and $\langle \alpha_D \rangle = 0.64 \pm 0.02$, where the angle brackets means that the values were obtained from \bar{D} and M_w instead of D and M . This is actually a calibration between \bar{D} and M_w . As expected for an extended polymer coil, α_D is larger than 0.6. With such a calibration, we could transfer $G(D)$ into a molecular weight distribution by using the following principle.

On the one hand, in the definition of $|g^{(1)}(t)|$, when $t \rightarrow 0$,

$$\begin{aligned} |g^{(1)}(t)|_{t \rightarrow 0} &= \langle E(t)E^*(0) \rangle_{t \rightarrow 0} \\ &= \int_0^\infty G(\Gamma) d\Gamma \propto I \end{aligned} \quad (5)$$

On the other hand, in the static LLS experiments, when $C \rightarrow 0$ and $\theta \rightarrow 0$, the net scattered intensity

$$I \propto \int_0^\infty f_w(M) M dM \quad (6)$$

where $f_w(M)$ is a weight distribution. A comparison of Eqs. (5) and (6) leads to

$$\begin{aligned} \int_0^\infty G(\Gamma) d\Gamma &\propto \int_0^\infty f_w(M) M dM \\ &\propto \int_0^\infty G(D) dD \end{aligned} \quad (7)$$

where we have changed Γ into D since $\Gamma = q^2 D$. In the spaces of $\log(M)$ and $\log(D)$, we can rewrite Eq. (7) as

$$\begin{aligned} \int_0^\infty G(D) D d \ln(D) \\ \propto \int_0^\infty f_w(M) M^2 d \ln(M) \end{aligned} \quad (8)$$

where $d \ln(D)$ can be replaced by $d \ln(M)$ since $D = k_D M^{-\alpha_D}$, which further leads to

$$f_w(M) \propto \frac{G(D) D}{M^2} \propto G(D) D^{1+2/\alpha_D} \quad (9)$$

It should be noted that in our above discussion we have omitted all proportional constants since they are irrelevant to a given distribution. From $f_w(M)$, we can calculate M_w by its definition,

$$\begin{aligned} (M_w)_{\text{calcd}} &= \frac{\int_0^\infty f_w(M) M dM}{\int_0^\infty f_w(M) dM} \\ &= \frac{k_D^{1/\alpha_D} \int_0^\infty G(D) dD}{\int_0^\infty G(D) D^{1/\alpha_D} dD} \end{aligned} \quad (10)$$

where we have used $dD \propto M^{-(\alpha_D+1)} dM$ on the basis of $D = k_D M^{-\alpha_D}$.

After replacing k_D and α_D in Eq. (10) with $\langle k_D \rangle$ and $\langle \alpha_D \rangle$, we obtained the values of $(M_w)_{\text{calcd}}$ for four chitosan. It was found that they are much lower than the measured M_w values from static LLS. This has not surprised us since $\langle k_D \rangle$ and $\langle \alpha_D \rangle$ obtained from those broadly distributed samples should be different from k_D and α_D for a set of monodisperse samples. For chitosan, it is very difficult to have a set of narrowly distributed standards with different molecular weights, but the same degree of deacetylation. In the past,⁹ we developed a method to obtain k_D and α_D , instead of $\langle k_D \rangle$ and $\langle \alpha_D \rangle$, from two or more broadly distributed samples. Just for the convenience of discussion, we outline this method in the following:

For two samples, we have two M_w from static LLS and two $G(D)$ from dynamic LLS, denoted as $M_{w,1}$, $M_{w,2}$, $G_1(D)$, and $G_2(D)$. On the basis of Eq. (10), we are able to obtain two calculated $(M_w)_{\text{calcd}}$, denoted as $(M_{w,1})_{\text{calcd}}$ and $(M_{w,2})_{\text{calcd}}$. The ratio of $(M_{w,1})_{\text{calcd}}$ to $(M_{w,2})_{\text{calcd}}$ is

$$\begin{aligned} \frac{(M_{w,1})_{\text{calcd}}}{(M_{w,2})_{\text{calcd}}} &= \frac{\left[\int_0^\infty G_1(D) dD \right] \left[\int_0^\infty G_2(D) D^{1/\alpha_D} dD \right]}{\left[\int_0^\infty G_2(D) dD \right] \left[\int_0^\infty G_1(D) D^{1/\alpha_D} dD \right]} \end{aligned} \quad (11)$$

Two calculated $(M_w)_{\text{calcd}}$ values should equal the two measured M_w values from static LLS. This implies that the left side of Eq. (11) can be replaced by $M_{w,1}/M_{w,2}$. Therefore, there exists only one unknown parameter α_D in Eq. (11). With a proper choice of α_D , we will be able to minimize the difference between the two sides of Eq. (11). For N samples, we can define two error functions as

$$\text{ERROR}(\alpha_D) = \sum_{i=1, j=1}^N \left[\frac{M_{w,i}}{M_{w,j}} - \frac{(M_{w,i})_{\text{calcd}}}{(M_{w,j})_{\text{calcd}}} \right]^2 \quad (12)$$

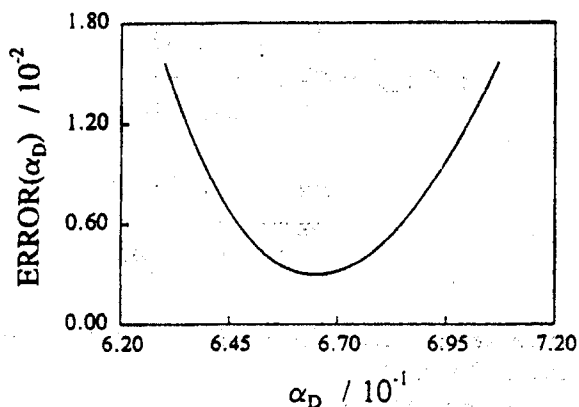


FIGURE 5 Typical plot of $\text{ERROR}(\alpha_D)$, where the minimum value of $\text{ERROR}(\alpha_D)$ corresponds to $\alpha_D = 0.665$ [see text for the definition of $\text{ERROR}(\alpha_D)$].

and

$$\text{ERROR}(k_D) = \sum_{k=1}^N [M_{w,k} - (M_{w,k})_{\text{calcd}}]^2 \quad (13)$$

By iterating α_D , we can first find a value of α_D to minimize $\text{ERROR}(\alpha_D)$; and then with this α_D , we can iterate k_D to minimize $\text{ERROR}(k_D)$. Now, we have to ask whether α_D and k_D calculated in this way are well defined.

Figures 5 and 6 show typical plots of $\text{ERROR}(\alpha_D)$ vs α_D and $\text{ERROR}(k_D)$ vs k_D , respectively. In Figure 5, there is a minimum of $\text{ERROR}(\alpha_D)$ at $\alpha_D = 0.665$. For each chosen α_D , Figure 6 shows that there is a well-defined minimum value of $\text{ERROR}(k_D)$. Considering both α_D

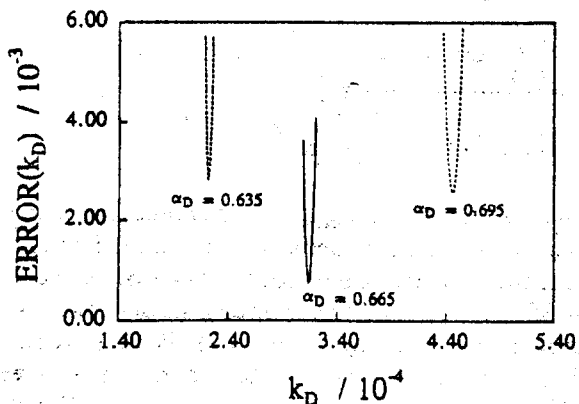


FIGURE 6 Typical plot of $\text{ERROR}(k_D)$, where the overall minimum value of $\text{ERROR}(k_D)$ corresponds to $\alpha_D = 0.665 \pm 0.015$ and $k_D = (3.14 \pm 0.20) \times 10^{-4}$ [see text for the definition of $\text{ERROR}(k_D)$].

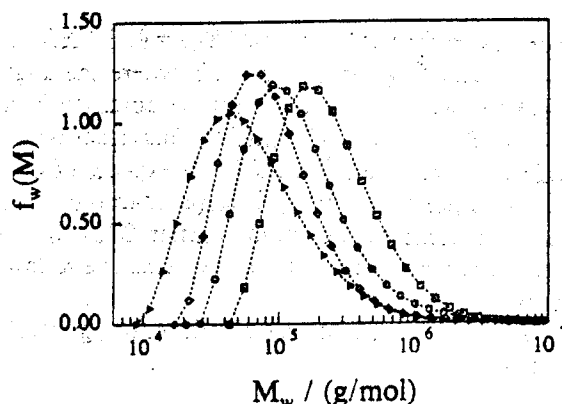


FIGURE 7 Four weight distributions calculated from $G(D)$. (\square) Chitosan 1, (\circ) chitosan 2, (\diamond) chitosan 3, and (Δ) chitosan 4 (see text for detail).

and k_D , there exists one overall minimum value of $\text{ERROR}(k_D)$. At this overall minimum point, $\alpha_D = 0.665$ and $k_D = 3.14 \times 10^{-4}$. It should be noted that α_D in Figure 5 is not as well-defined as k_D in Figure 6. After considering all experimental uncertainties, we have $\alpha_D = 0.665 \pm 0.015$ and $k_D = (3.14 \pm 0.20) \times 10^{-4}$. The paired values of α_D and k_D defines a calibration between D and M , which is plotted in Figure 4 by the dotted line. After having this calibration, we were ready to convert $G(D)$ into $f_w(M)$.

Figure 7 shows four weight distributions $f_w(M)$ of chitosan 1 (\square), chitosan 2 (\circ), chitosan 3 (\diamond), and chitosan 4 (∇), respectively. On the basis of these four distributions, we were able to calculate $(M_z)_{\text{calcd}}$, $(M_w)_{\text{calcd}}$, and $(M_n)_{\text{calcd}}$. The values of $(M_w)_{\text{calcd}}$, $(M_w)_{\text{calcd}}/M_w$, and the calculated polydispersity index $(M_z:M_n)_{\text{calcd}}$, $(M_w:M_n)_{\text{calcd}}$ are summarized in Table II. Chitosan 1 has a narrower molecular weight distribution, which is reasonable since the hydrolytic degradation of chitosan 1 should produce a certain amount of low molecular weight species. This is why the main difference in the four distribution is in the range of low molecular weight, which leads to a big difference in $M_z:M_n$.

Before we conclude this study, it should be pointed out that at higher concentration, chitosan, especially those samples with higher molecular weight, will form larger aggregates even in $0.2M$ $\text{CH}_3\text{COOH}/0.1M$ CH_3COONa aqueous solution. It seems that this type and amount of low molecular weight electrolytes is not able to completely eliminate the polyelectrolyte effect and hydrogen bonding between different chitosan chains.

Figure 8 shows a typical diffusion coefficient

Table II M_w and the Polydispersity Index $M_z:M_w:M_n$ of Four 91% Deacetylated Chitosans Calculated from $G(D)$ by Using the Calibration of $D = 3.14 \times 10^{-4} M^{-0.665}$

Sample	$10^{-5} (M_w)_{\text{calcd}}$ (g/mol)	$(M_z:M_n)_{\text{calcd}}$	$(M_w/M_n)_{\text{calcd}}$	$(M_w)_{\text{calcd}}/M_w$
Chitosan 1	3.45	8.02:1.00	1.98:1.00	1.00
Chitosan 2	2.43	23.9:1.00	2.38:1.00	0.99
Chitosan 3	1.60	29.0:1.00	2.33:1.00	1.02
Chitosan 4	1.05	20.7:1.00	2.41:1.00	0.99

distribution $G(D)$ of chitosan 2 at $\theta = 45^\circ$ and $C = 1.15$ mg/mL, where the peak with a lower D value represents the larger aggregates. Since $G(D)$ is a z - or an intensity-weighted distribution, i.e., $G(D) \propto \int_n(M)M^3$ in the logarithmic space, the larger area under the peak with a lower D value actually represents a very small amount of aggregate in terms of number. This small amount of aggregate has been overlooked in other types of experiments, such as in viscometry and even in static LLS, which leads to a larger weight average molecular weight (W. Wang, unpublished results). This might partially explain that α_n (0.880) in the reported Mark-Houwink equation is lower in comparison with the value of α_D (0.665), where α_D and α_n are related by $\alpha_D = (1 + \alpha_n)/3$ according to Flory.²¹ In our future study, special caution will have to be taken when we characterize chitosan in aqueous solution. In order to avoid the aggregation, a very dilute solution has to be used.

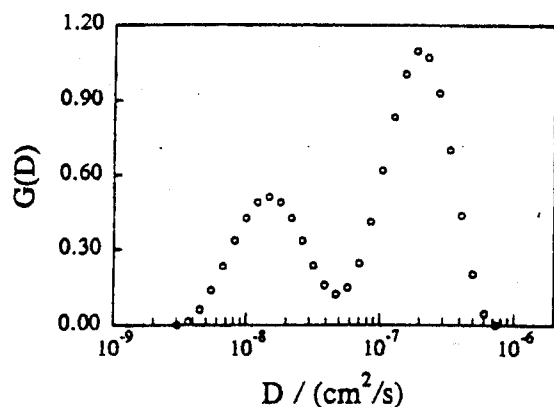


FIGURE 8 Typical diffusion coefficient distribution $G(D)$ of chitosan 2 at $\theta = 45^\circ$ and higher concentration ($C = 1.15$ g/mL), where the peak located at the lower D side represents larger aggregates.

CONCLUSION

Four 91% deacetylated chitosans, a kind of poly-electrolyte, have been successfully studied by a combination of dynamic and static laser light scattering in $0.2M$ $\text{CH}_3\text{COOH}/0.1M$ CH_3COONa aqueous solution. Both our dynamic and static light scattering results consistently show that chitosan has an extended chain conformation and a tendency to aggregate in aqueous solution even in the presence of a certain amount of low molecular weight electrolytes. In this study, we have established a calibration between molecular weight (M) and the translational diffusion coefficient (D), i.e., $D = 3.14 \times 10^{-4} M^{-0.665}$, which leads to another way of characterizing not only the weight average molecular weight of chitosan, but also its molecular weight distribution. It is worth addressing that as long as the characterization is carried out in the same solvent and at 25°C , this established calibration between D and M should hold no matter what kind of laser light scattering spectrometer will be used.

The financial support of this work by the RGC (the Research Grants Council of Hong Kong Government) Earmarked Grant 1993/94 (CUHK 79/93E, 221600140) is gratefully acknowledged.

REFERENCES

1. Sandford, P. A. & Steignes, A. (1991) *ACS Symp. Ser.* 467, 430, and references therein.
2. Wang, W., Qin, W. (1991) *Makromol. Chem. Rapid Commun.* 12, 559.
3. Roberts, G. A. F. & Domszy, J. G. (1982) *Int. J. Biol. Macromol.* 4, 37.
4. Nordtveit, R. J., Varum, K. M. & Smidsrød, O. (1994) *Carbohydr. Polym.* 23, 253.

5. Wang, W., Bo, S., Li, S. & Qin, W. (1991) *Int. J. Biol. Macromol.* **13**, 281.
6. Varum, K. M., Anthonsen, M. W., Grasdalen, H. & Smidsrød, O. (1991) *Carbohydr. Res.* **217**, 19.
7. Varum, K. M., Anthonsen, M. W., Grasdalen, H. & Smidsrød, O. (1991) *Carbohydr. Res.* **211**, 17.
8. Wu, C. (1993) *Macromolecules* **26**, 3821.
9. Wu, C. (1994) *J. Polym. Sci. Polym. Phys.* **32**, 803.
10. Zimm, B. H. (1948) *J. Chem. Phys.* **16**, 1099.
11. Chu, B. (1974) *Laser Light Scattering*. Academic Press, New York.
12. Pecora, R. (1976) *Dynamic Light Scattering*. Plenum Press, New York.
13. Stockmayer, W. H. & Schmidt, M. (1982) *Pure. Appl. Chem.* **54**, 407.
14. Stockmayer, W. H. & Schmidt, M. (1984) *Macromolecules* **17**, 509.
15. Terayama, H. (1952) *J. Polym. Sci.* **8**, 243.
16. Miya, M., Iwamoto, R., Kawa, R. & Mima, S. (1980) *Int. J. Biol. Macromol.* **2**, 323.
17. Wu, C. & Xia, K. Q. (1993) *Rev. Sci. Instr.* **65**, 587.
18. Fujita, H. (1988) *Macromolecules* **21**, 179.
19. Anthonsen, M. W., Varum, K. M. & Smidsrød, O. (1993) *Carbohydr. Polymers* **22**, 193.
20. Wu, C. (1993) *Colloid Polym. Sci.* **271**, 947.
21. Flory, P. J. (1953) *Principles of Polymer Chemistry*. Cornell University Press, Ithaca, NY.